Studies on the stability of a $La_{0.8}Pr_{0.2}NiAl_{11}O_{19}$ catalyst for syngas production by CO_2 reforming of methane

Yan Liu [a], Tiexin Cheng [a], Dongmei Li [b], Pengbo Jiang [a], Junxia Wang [a], Wenxing Li [a], Yingli Bi [a], and Kaiji Zhen [a,*]

[a] College of Chemistry, Jilin University, Changchun 130023, PR China
[b] National Laboratory of Super Hard Materials, Jilin University, Changchun 130023, PR China

Received 2 July 2002; accepted 27 September 2002

CO_2 reforming of CH_4 was studied over a magnetoplumbite-type hexaaluminate $La_{0.8}Pr_{0.2}NiAl_{11}O_{19}$ catalyst, which showed very high activity for over 300 h without deactivation at 1023 K. This catalyst showed good resistance to carbon deposition, which in this reaction and in CH_4 decomposition was investigated by means of XPS and TEM. It is suggested that nano-tube-like carbon is an intermediate in this reaction and a spillover of carbon from crystalline Ni onto the hexaaluminate oxide occurred during the reaction.

KEY WORDS: methane; CO_2 reforming; hexaaluminate; catalysis.

1. Introduction

With the requirements of environmental protection, the reaction of CH_4 reforming with CO_2 has recently attracted renewed interest [1–3], and is useful for the utilization of carbon source in exhaust and producing synthesis gas with a H_2/CO ratio of around 1, which is needed for F-T synthesis or oxo-synthesis. As is well known, the precious metals Rh, Ru, Pd, Pt and Ir have successfully been employed as highly active catalysts for this reaction; however, their high price renders their industrial use questionable. Supported Ni catalysts have been reported to be the first generation of effective Ni-based catalysts for the reaction [4], although they deactivate very easily due to carbon deposition, nickel sintering and phase transformation. Therefore, the development of a new generation of active and stable nickel-based catalysts is of great importance for their practical application to the petrochemical and chemical refining industry. Addition of alkaline earth and rare earth oxides to Ni-based catalysts is effective in increasing the resistance to carbon deposition on the catalyst for a duration of 100 h [5,6], which suggests a possibility for improving the performance of nickel-based catalysts.

It is known that CH_4 decomposition and CO disproportionation take place in the CO_2 reforming of methane, and these reactions are the possible routes for carbon deposition. It has been reported that the surface active carbon originates from methane and that accumulation of the less active carbon causes catalyst deactivation as suggested in a ^{13}C labeling study [7]. The common types of deposited carbon are whisker-like carbon, encapsulating carbon and pyrolytic carbon [8].

Numerous authors [9,10] have presented calculations predicting the thermodynamic potential of graphitic carbon deposition as a function of operating conditions using reaction mixtures containing CH_4, CO_2, H_2 and H_2O. The results drawn from their calculations suggest operation at high temperature (1000 K), and with CO_2/CH_4 ratios higher than unity in order to avoid carbon deposition; however, from an industrial standpoint, it may be desirable to carry out this reaction at lower temperature with CO_2/CH_4 ratios near unity. This requires the use of a reforming catalyst, which incorporates a kinetic inhibition of carbon deposition under conditions thermodynamically favorable for carbon deposition.

The present authors have reported two series of hexaaluminates $ANiAl_{11}O_{19-\delta}$ (A = Ca, Sr, Ba and La) and $LaNi_yAl_{12-y}O_{19-\delta}$ ($y = 0.3$, 0.6, 0.9 and 1.0) as a new generation of catalysts for CO_2 reforming of methane to synthesis gas, in which the active component Ni ions are inlaid in the hexaaluminate lattices to substitute for part of the Al ions [11,12]. Interaction of Ni particles that are formed during the reduction and the hexaaluminate oxides can stabilize small Ni crystallites and increase catalyst lifetime by decreasing carbon deposition. Based on their previous work, the present authors prepared $La_{0.8}Pr_{0.2}NiAl_{11}O_{19}$ by substituting some La ions for Pr ions. These catalysts exhibited high catalytic activity and stability, providing over 89 and 91% conversion of CH_4 and CO_2, respectively, which remained unchanged for 300 h on-stream time and even longer.

The aim of this paper is to find the reason for the low amount of carbon deposited over $La_{0.8}Pr_{0.2}NiAl_{11}O_{19}$ in methane reforming with CO_2 at 750 °C.

* To whom correspondence should be addressed.
E-mail: zkj@mail.jlu.edu.cn

1011-372X/03/0100-0101/0

2. Experimental

2.1. Catalyst preparation

Nitrates of lanthanum, potassium, nickel and aluminum were dissolved in distilled water with a molar ratio of 0.8:0.2:1:11, respectively. The aqueous solution was then slowly added to a polyethylene glycol–isopropyl alcohol solution under magnetic stirring. The mixture was evaporated to dryness at 80 °C, followed by removal of the dispersant and decomposition of the nitrates in an oven. After being ground to a fine powder, the sample was calcined at 400 °C for 2 h, followed by calcination at 1250 °C for 5 h in a muffer furnace.

2.2. Catalyst characterization

X-ray diffraction (XRD) patterns of the samples obtained using a Shimadzu XD-3A diffractometer with CuKα radiation at 30 kV and 20 mA were used to identify the major phase present in the calcined catalysts.

The deposited carbon on the $La_{0.8}Pr_{0.2}NiAl_{11}O_{19}$ catalyst was characterized by X-ray photoelectron spectroscopy (XPS; VG ESCA Mark II) using AlKα radiation; the analyzer was operated at a pass energy of 50 eV and a step size of 0.05 eV. The C_{1s} peak of the contaminating carbon at 284.6 eV was used as internal standard. The sample probe was transferred using a glove box filled with N_2 of high purity to prevent the samples from contacting atmospheric O_2 and H_2O. The amount of carbon deposited on the catalysts was determined using a thermogravimetric analyzer (TGA; Perkin-Elmer TGA7).

Transmission electron microscopy (TEM) images of the deposited carbon were obtained using a Hitachi-8100IV electron microscope operated at 200 kV. The sample was treated with CH_3CH_2OH and then dispersed by ultrasonics in an aqueous surfactant solution before being mounted on a copper grid.

2.3. Catalytic properties test

The reforming reaction was carried out under atmospheric pressure at 1023 K in a tubular fixed-bed quartz reactor with an inner diameter of 8 mm. The reactant mixture consisted of CH_4 and CO_2 with a molar ratio of 1:1 and flowing at a rate of 30 ml/min. An amount of 0.2 g of catalyst was embedded in each run. Before the reaction the catalyst was reduced at 900 °C in a flow of 10% H_2/Ar gas mixture for 40 min. Exit gases (reactant/product mixtures) were analyzed by a gas chromatograph (Shimadzu GC-8A) equipped with a thermal conductivity detector (TCD) and Porapak-Q and 5A molecular sieve columns.

3. Results and discussion

3.1. Catalytic properties

Data for the catalytic properties at 1023 K are shown in figure 1, indicating that in the first hour CH_4 conversion (90.5%) is slightly higher than that (88.3–89.8%) in the following time-on-stream (TOS), which would be due to decomposition of CH_4 molecules to carbon-containing species. In the meantime, the CO_2 conversion changed

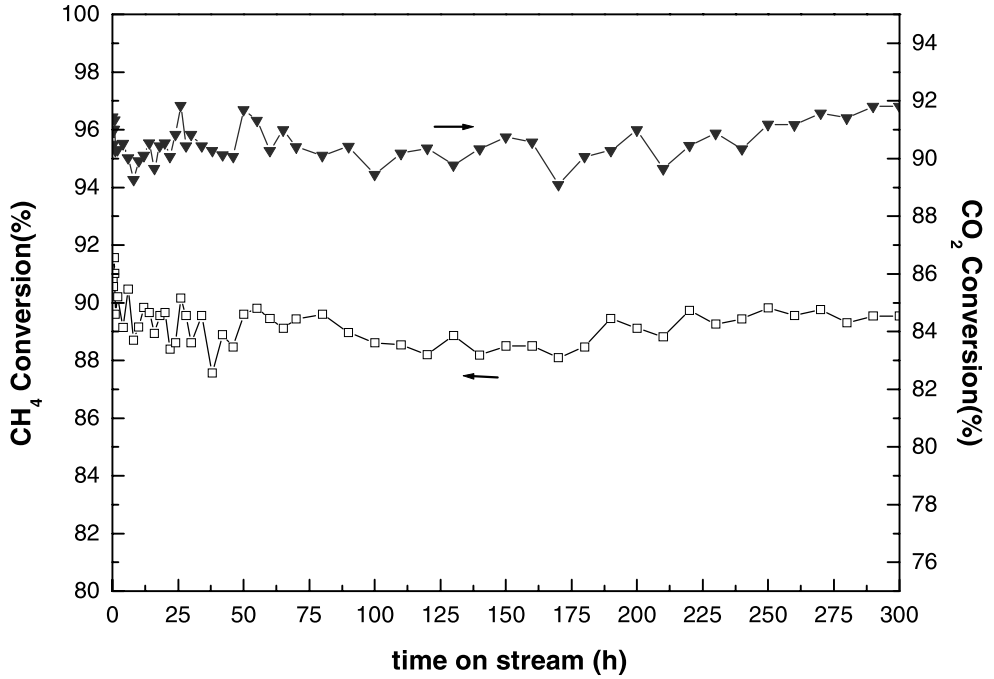

Figure 1. Catalytic activity and stability of $La_{0.8}Pr_{0.2}NiAl_{11}O_{19}$ catalysts for CH_4 reforming with CO_2 at 1023 K with $CH_4/CO_2 = 20\,ml/20\,ml$.

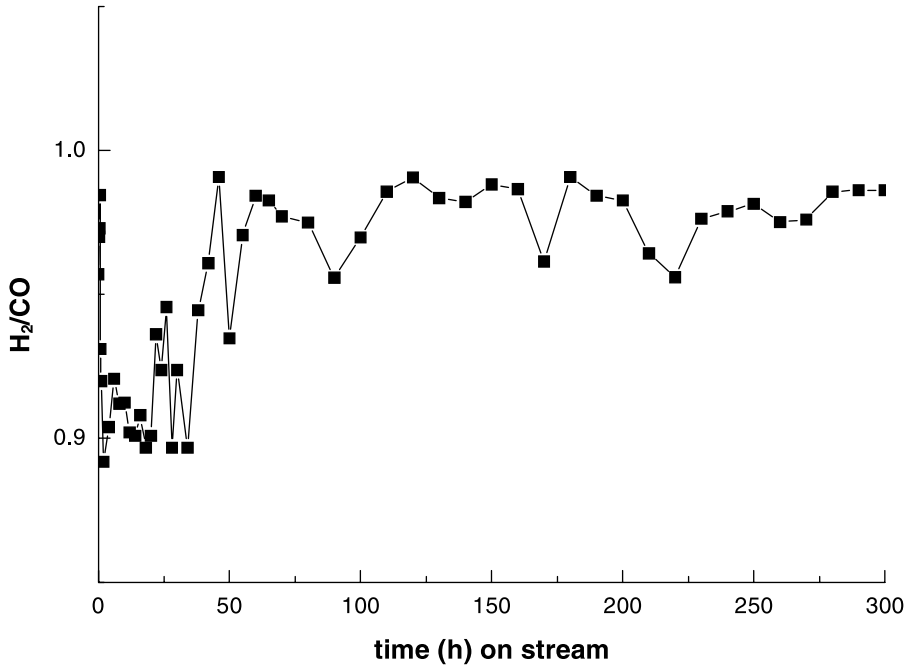

Figure 2. Change of H_2/CO with reaction time on stream over the $La_{0.8}Pr_{0.2}NiAl_{11}O_{19}$ catalyst.

between 89.5 and 91.5%. No deactivation is detected within 300 h of TOS. After 250 h of TOS, the conversions of CH_4 and CO_2 were stabilized at 89 and 91%, respectively. These data approached the equilibrium ones of the reaction [13]. In a recent report of Slagtern *et al.*, the catalytic performance of the La–Ni–Al–O hexaaluminate catalyst for this reaction in a fluid-bed reactor at 1073 K has been published [14]. Although their results cannot be compared with those obtained in the present paper due to very different conditions adopted in both works, it is worth emphasizing that the conversion of methane over our catalyst is 89%, about 30% higher than that reported by Slagtern *et al.*

Figure 2 shows the change of H_2/CO ratio over this catalyst with TOS. It is interesting to note that this ratio reached 0.98 in the first hour, then decreased to 0.9 in the following 20 h. Within the following 18 h, the ratio changed in an oscillating mode between 0.89 and 0.92, indicating a periodic cycle of carbon deposition and elimination. After 50 h of TOS, the ratio stabilized at 0.97, indicating that carbon deposition and elimination occurred simultaneously. The reason for the extremely stable catalytic performance of this catalyst is the comparable velocities of carbon deposition and elimination by CO_2.

The excess of CO in the syngas produced may be caused by a reverse water-gas shift reaction ($CO_2 + H_2 \rightarrow CO + H_2O$), which reduces the amount of hydrogen in the product. To prove this, ice-water was placed downstream of the reactor to condense the water vapor produced in the reaction for 24 h. The condensed water gave a measurement of the approximately average rate of water formation, which is around 0.01 g per hour. Over this catalyst, the H_2/CO ratio stabilized at 0.9 in the first 24 h TOS and increased to 0.96 after 50 h TOS, indicating that the reverse water-gas shift occurs at the beginning of the reaction over the fresh catalyst.

Decomposition of CH_4 over the catalyst produces hydrogen and carbon species, part of which reacts with oxygen atoms of CO_2 to produce CO. Table 1 shows the amounts of carbon deposited on $La_{0.8}Pr_{0.2}NiAl_{11}O_{19}$ in relation to reaction time at 750 °C in CH_4/CO_2 mixture, which increased gradually with time and reached a constant value after 2 h probably due to the reaction equilibrium.

3.2. Crystal structure of the catalysts

Figure 3(a) shows the principal XRD characteristic peaks of the magnetoplumbite-type $La_{0.8}Pr_{0.2}NiAl_{11}O_{19}$ hexaaluminates before reaction ($2\theta = 32.12^\circ$, 33.14° and 36.14°). The crystal structure of the hexaaluminates obtained is consistent with that of the samples synthesized in our previous work [9,10]. Diffractograms (figures 3(c) and (d)) of the catalyst after 0.5, 2, 24 and

Table 1
Carbon weight vs. reaction time

TOS (h)	1	2	12	24	60	300
Coke (g/g cat%)	0.48	0.78	0.91	0.8	0.79	0.75

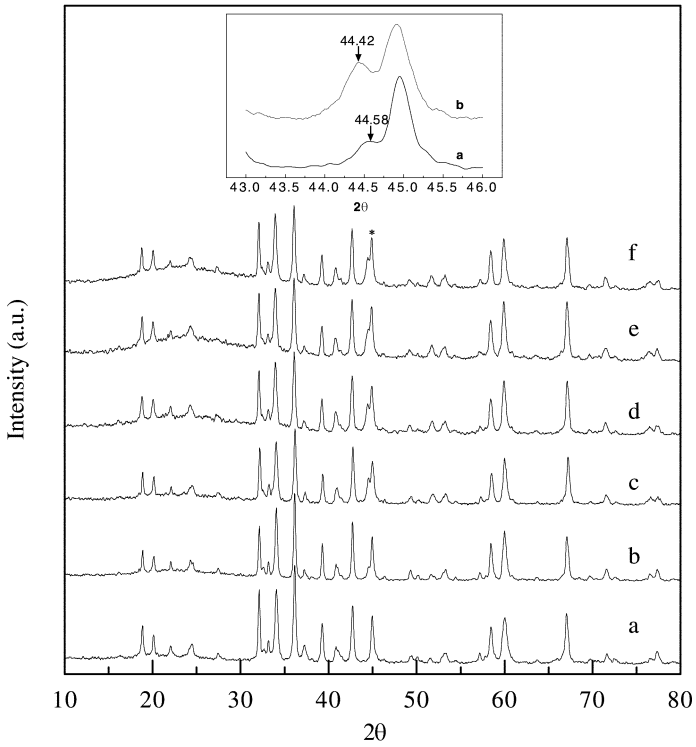

Figure 3. XRD patterns of $La_{0.8}Pr_{0.2}NiAl_{11}O_{19}$ (a); after reduction (b); and reaction for 0.5 (c), 2 (d), 24 (e) and 300 (f) h.

300 h of TOS showed no obvious change in the phase composition and crystal structure. A peak at 44.5° for metallic Ni^0 (111) can be clearly observed after reduction of the catalysts, as shown in figure 3(b), indicating that a large fraction of nickel atoms is produced and separated from the hexaaluminate lattice to form an individual metallic phase. However, in the patterns of samples after reaction for different TOS a 0.16° shift of 2θ towards higher angle and a weak intensity of the peak for Ni (111) can be observed (inset of figure 3), owing to dissolution of some carbon atoms (or species) into the nickel crystallite, to form Ni(C) according to Slagtern *et al.* [14]. The peak intensities of Ni(C) increase with increasing reaction time within the first 2 h and do not change in the range 2–300 h, meaning that the structure of Ni(C) is also stable during the reaction process. This result indicates that carbon is deposited predominantly on the nickel particles.

Figures 4(a) and (b) show the TEM profiles of $La_{0.8}Pr_{0.2}NiAl_{11}O_{19}$ before H_2 reduction and an enlarged view, respectively. The former illustrates the stick structure of the typical hexaaluminate and the latter represents details of the crystallite as hexagonal planar of about 0.5 nm thickness, which is one-tenth of their width. The planar morphology of the hexaaluminate crystal reflects a layered structure. The flat facet orientation is parallel to the *b* axis. For this anisotropic [15] shape of crystallites, the crystal growth of hexaaluminate along the *c* axis is strongly suppressed, and the growth along the *a* axis is similarly suppressed due to a large ratio of length to width.

3.3. Carbon deposition

Figures 5(a) and (b) show the TEM profiles of $La_{0.8}Pr_{0.2}NiAl_{11}O_{19}$ after H_2 reduction at 1173 K and 300 h reaction at 1023 K, respectively. The bulk structure of the used catalyst does not change compared with that of the fresh catalyst. From figure 5(a), it can be seen that some nano-tube-like carbon with an average diameter of 20–30 nm is formed, and on it there are some nickel particles. Besides, we also observed encapsulating carbon and a few nickel particles wrapped in it. The particle size of the nickel crystallite and the bulk structure of the samples do not change even after 300 h of reaction. The diameter of the nano-tube-like carbon and nickel particles on $La_{0.8}Pr_{0.2}NiAl_{11}O_{19}$ seems to be smaller than that on $LaNiAl_{11}O_{19}$ [16]. This result indicates that the aggregation of nickel particles on the $La_{0.8}Pr_{0.2}NiAl_{11}O_{19}$ catalyst is more difficult than that on the $LaNiAl_{11}O_{19}$ catalyst due to the interaction between the metallic nickel and hexaaluminate oxide [17]. This may be the reason for $La_{0.8}Pr_{0.2}NiAl_{11}O_{19}$ having relatively higher stability toward sintering and carbon deposition.

It is also demonstrated that the nano-tube-like carbon was the predominant form of carbon during CH_4 decomposition (figure 6(a)), which is as reported previously [18,19]. It is known that this kind of carbon does not cause deactivation of the catalyst. From figure 6(b), it is seen that the nano-tube-like carbon can be eliminated rapidly by CO_2, while the encapsulating carbon still exists even after reaction with CO_2 for 40 min. Kroll

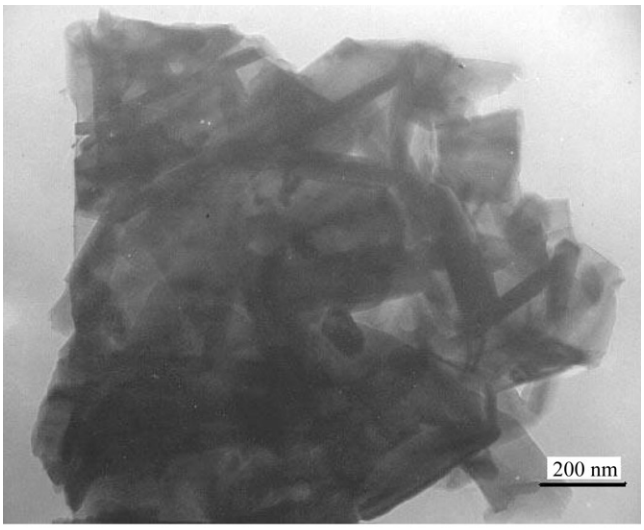

(a)

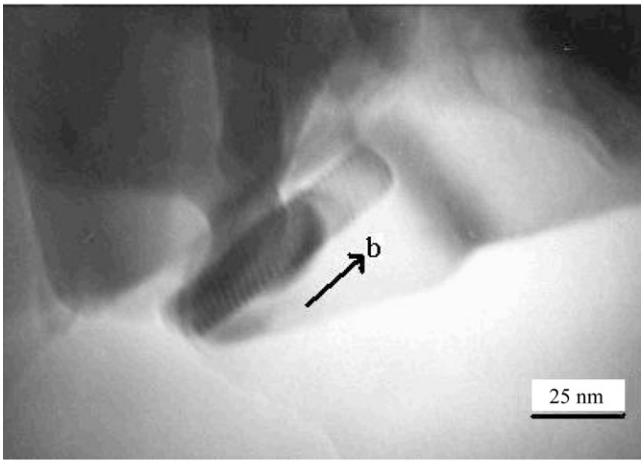

(b)

Figure 4. TEM image of fresh catalyst (a) and enlarged view (b).

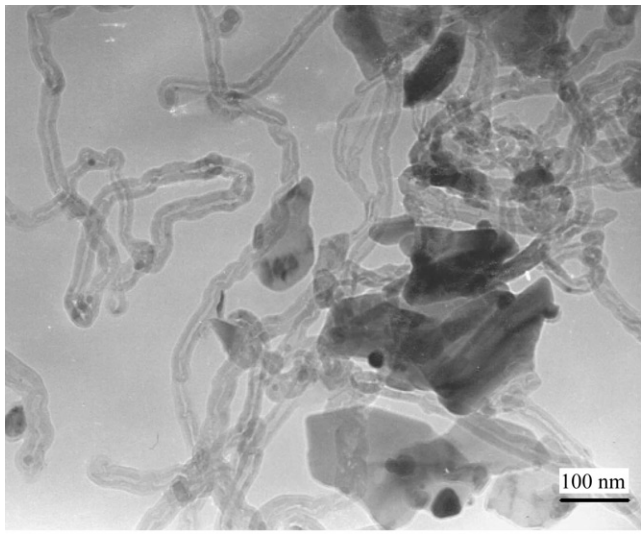

(a)

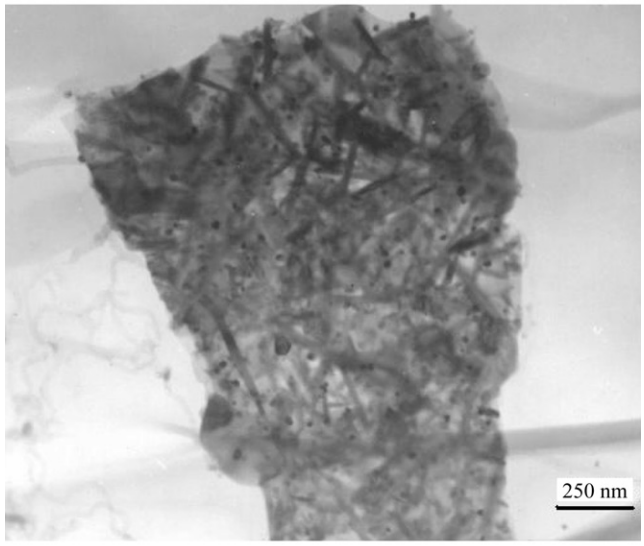

(b)

Figure 5. TEM images of the catalyst after 300 h TOS.

et al. [20] considered that the form of the nickel particles determines the type of carbon formed: faceted and flat particles produce filamentous carbon and small, spherical particles produce encapsulating carbon [21].

Figure 7 shows XPS spectra of C_{1s} of the samples treated under different conditions: (a) reduced in H_2 at 1173 K for 40 min then contacted with CH_4/CO_2 at 1023 K for 300 h; (b) after reduction in H_2 and contacted with CH_4 for 1 h; and (c) sample of (b) reacted with CO_2 for 20 min. It is clear that three kinds of carbon species were formed on H_2–CH_4/CO_2 (figure 7(a)) and H_2–CH_4 (figure 7(b)) treated catalyst surfaces, respectively. A peak at 282.9 eV is due to carbide carbon [22], a peak at 285.5 eV is assigned to graphitic carbon [23] and a peak at 284.6 eV is attributed to contaminated carbon used as internal standard. The peak intensity of carbide on the H_2–CH_4 treated surface is much stronger than that on the H_2–(CH_4/CO_2) one, implying that the interaction of the surface carbide carbon with oxygen atoms to form CO occurred on the H_2–(CH_4/CO_2) treated catalyst surface. A remarkable difference between H_2–(CH_4/CO_2) and H_2–CH_4/CO_2 (figure 7(c)) treated catalyst surfaces was that no surface C_{1s} peak at ~282.9 eV is detected on the CO_2 treated sample. A new C_{1s} peak at 288.8 eV observed on the CO_2 treated catalyst surface is probably due to the formation of carbon–oxygen species. The results revealed that the reaction of the surface carbide with adjacent oxygen atoms dissociated from CO_2 to CO was a fast step. A conclusion can be drawn that oxygen atoms dissociated from CO_2 by metallic nickel are able to react quickly with their adjacent carbide carbon to form CO. Comparing the XPS results with the data of the TEM characterization, we can conclude that the peak at 282.9 eV is attributed to nano-tube-like carbon and the peak at 285.5 eV to the encapsulating carbon.

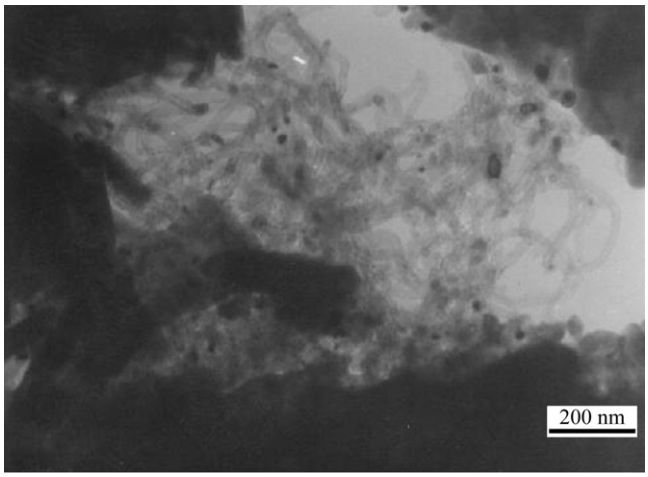

(a)

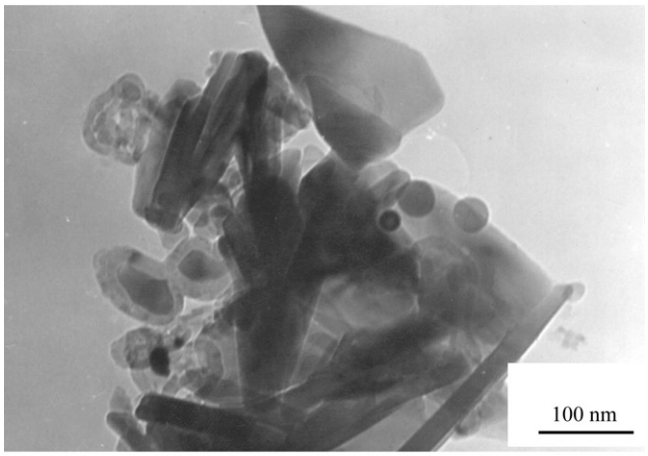

(b)

Figure 6. TEM image after (a) reaction with CH_4 for 40 min and (b) (a) followed by reaction with CO_2 for 20 min.

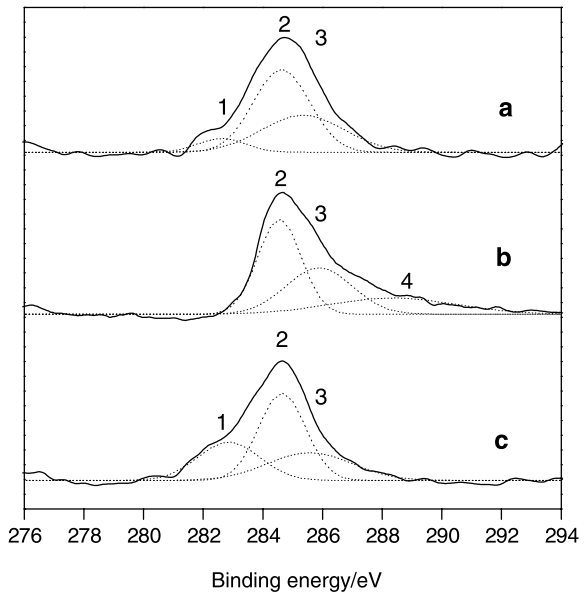

Figure 7. XPS spectra in C_{1s} region for $La_{0.8}Pr_{0.2}NiAl_{11}O_{19}$ after (a) CH_4/CO_2 (1023 K, 300 h); (b) CH_4 (1173 K, 40 min) → CO_2 (1173 K, 20 min); (c) CH_4 (1173 K, 40 min).

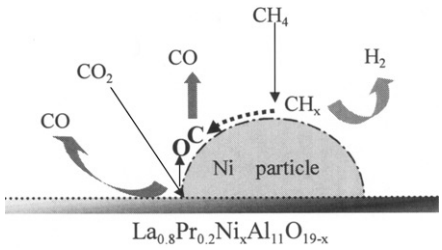

Figure 8. Schematic representation of the CO_2 reforming of methane over the $La_{0.8}Pr_{0.2}NiAl_{11}O_{19}$ catalyst.

3.4. Reaction mechanism

Although this nickel-based catalyst is very stable and active for the reaction under investigation, the CO_2 reforming of methane still follows a commonly accepted mechanism, as shown in figure 8. In the case of $La_{0.8}Pr_{0.2}NiAl_{11}O_{19}$, the active carbon species is first formed on the metallic nickel surface via the activation of CH_4, followed by spillover of carbon onto the hexaaluminate oxide surface, and the spiltover carbon species can be removed by reaction with CO_2 rapidly before converting to nano-tube-like carbon.

Snoeck *et al.* reported that the carbon whisker formation rate on supported Ni catalysts is determined by the diffusion rate of NiC through the Ni cluster, and that this diffusion rate is proportional to the radius of each Ni cluster [24]. Meanwhile Audier *et al.* [25–27] found that the orientation of conical nickel particles on the tips of the whiskers depends on the type of crystallographic structure. It has been suggested that carbon atoms, formed by CH_4 decomposition on the Ni (100) and Ni (110) surfaces, diffuse across the nickel particle surface and by deposition on the Ni (111) surfaces form ordered graphite layers aligned parallel to the metal–carbon interface [28]. This finding supports our interpretation that carbon species migrate to the subsurface of the catalyst to form bulk-like NiC nickel as shown in figure 3.

From TEM and XPS measurements, it is also found that the nano-tube-like carbon can be eliminated by CO_2, indicating this carbon is an intermediate in this reaction. We assume that nano-tube-like carbon deposited on the catalyst is specifically reactive in the formation of CO.

4. Conclusion

The reduced $La_{0.8}Pr_{0.2}NiAl_{11}O_{19}$ exhibited stable activities for CH_4 reforming with CO_2 and no deactivation was detected even after 300 h of reaction. The carbon deposited on the catalyst was produced by CH_4 decomposition during the reaction. There are two kinds of deposited carbon produced by CH_4 decomposition: carbide carbon formed by nano-tube-like carbon is the intermediate in this reaction and graphitic carbon

formed by encapsulating carbon which wraps some nickel particles is difficult to be eliminated, which is the predominant form of the deposited carbon.

Acknowledgment

The authors gratefully acknowledge the Natural Science Foundation Committee of China for financial support (29973012).

References

[1] J.R. Rostrup-Nielsen and J.H. Bak Hansen, J. Catal. 144 (1993) 38.
[2] S.M. Stagg, E. Romeo, C. Padro, and D.E. Resasco, J. Catal. 178 (1998) 137.
[3] Guolin Xu, Keying Gao, Hengyong Xu and Yongde Wei, J. Mol. Catal. 147 (1999) 47.
[4] Li Wengying, Feng Jie and Xie Kechang, React. Kinet. Catal. Lett. 64 (1998) 381.
[5] J.R. Rostrup-Nielsen, Stud. Surf. Sci. Catal. 36 (1988) 73.
[6] T. Horiuchi, K. Sakuma, T. Fuk, Y. Kubo, T. Osaki and T. Mori, Appl. Catal. 144 (1996) 111.
[7] H.M. Swaan, V.C.H. Kroll, G.A. Martin and C. Mirodatos, Catal. Today 21 (1994) 571.
[8] J.R. Rostrup-Nielsen, in: *Catalysis Science and Technology*, Vol. 5, eds. J.R. Anderson and M. Boudart (Springer-Verlag, New York, 1984).
[9] R.E. Reitmeier, M.A. Benner and H.M. Baugh, Ind. Eng. Chem. 40 (1948) 620.
[10] G.A. White, T.R. Roszkowski and D.W. Stanbrige, Hydrocarbon Process. 54 (1975) 130.
[11] Zhanlin Xu, Ming Zhen, Yingli Bi and Kaiji Zhen, Catal. Lett. 64 (2000) 157.
[12] Zhanlin Xu, Ming Zhen, Yingli Bi and Kaiji Zhen, Appl. Catal. 198 (2000) 267.
[13] M.C.J. Bradford and M.A. Vannice, Catal. Rev. Sci. Eng. 41 (1999) 1.
[14] Á. Slagtern, U. Olsbye, R. Blom, I.M. Dahl and H. Fjellvag, Appl. Catal. A 145 (1996) 375.
[15] F. Laville, M. Perrin, A.M. Lejus, M. Gasperin, R. Moncorge and D. Vivien, J. Sol. State Chem. 65 (1986) 301.
[16] Liu Yan, Xu Zhanlin, Cheng Tiexin, Zhou Guangdong, Yingli Bi and Kaiji Zhen, Kinet. Catal. (in press).
[17] N.M. Rodriguez, J. Mater. Res. 8 (1993) 3233.
[18] C.H. Burtholomew, Catal. Rev. Sci. Eng. 24 (1982) 67.
[19] D.L. Timm, Catal. Rev. Sci. Eng. 16 (1982) 155.
[20] V.C.H. Kroll, H.M. Swann and C. Mirodatos, J. Catal. 161 (1996) 409.
[21] R.A. Cabrol and A. Oberlin, J. Catal. 89 (1984) 256.
[22] E.O.F. Zdansky, A. Nilsson and N. Martensson, Surf. Sci. 301 (1994) L583.
[23] Lu Yong, Yu Changchun, Liu Yu and Shen Shikong, Chem. Lett. 6 (1997) 515.
[24] J.W. Snoeck, G.F. Froment and M. Fowles, J. Catal. 169 (1997) 240.
[25] M. Audier, A. Oberlin, M. Oberlin, M. Coulon and L. Bonnetain, Carbon 19 (1981) 217.
[26] M. Audier, M. Coulon and A. Oberlin, Carbon 18 (1980) 73.
[27] M. Audier, A. Oberlin and M. Coulon, J. Cryst. Growth 55 (1981) 549.
[28] V.V. Chesnokov, V.I. Zaikovskii, R.A. Buyanov, V.V. Molchanov and L.M. Plyasova, Catal. Today 24 (1995) 265.